

Supporting Information

Lanthanoid containing phosphotungstates: Syntheses, crystal structure, electrochemistry, photoluminescence and magnetic properties

List of figures and table contents

Table S1. Crystallographic table of polyanions $K_{11}[Ln(PW_{11}O_{39})_2] \cdot xH_2O$ ($Ln = Pr^{3+}$ (1a), Nd^{3+} (2a), Eu^{3+} (3a), Tb^{3+} (5a), Dy^{3+} (6a), Er^{3+} (8a), and Tm^{3+} (9a)) crystallized in the monoclinic system.

Table S2. Bond lengths of Ln-O for polyanions $K_{11}[Ln(PW_{11}O_{39})_2] \cdot xH_2O$ ($Ln = Pr^{3+}$ (1a), Nd^{3+} (2a), Eu^{3+} (3a), Gd^{3+} (4a), Tb^{3+} (5a), Dy^{3+} (6a), Ho^{3+} (7a), Er^{3+} (8a), and Tm^{3+} (9a)).

Figure S3. FT-IR spectra of molecular cluster Pr(1a) – Yb(10a) (recorded in KBr).

Table S4. Vibrational frequencies of P-O and W-O bands of molecular cluster Pr(1a) – Yb(10a).

Figure S5. FT-IR spectra of Ce – Er complexes obtained from reaction of $[\alpha\text{-PW}_{11}O_{39}]^{7-}$ with lanthanoid metal salt (recorded in KBr).

Figure S6. Solid state UV/vis spectrum of molecular cluster Nd(2a).

Figure S7. Solid state UV/vis spectrum of molecular cluster Dy(6a).

Figure S8. Solid state UV/vis spectrum of molecular cluster Ho(7a).

Figure S9. Solid state UV/vis spectrum of molecular cluster Er(8a).

Table S10. Cathodic peak potentials, peak potential differences, formal redox potentials and cathodic peak potential differences with respect to the first reduction wave of (PW_{11}) .

Figure S11. Dependence of the peak current on the square root of the scan rate for the most positive redox couple of a 0.2 mM Tm(9a) solution in 1M $CH_3COOLi + CH_3COOH$, pH=5.

Figure S12. Comparison of the cyclic voltammograms obtained from solution of conc. 2×10^{-4} M for Eu(3a) – Tm(9a) in 1M $LiCH_3COO/CH_3COOH$, pH=4.0 at $10mV.s^{-1}$.

Figure S13. Photoluminescence spectrum of molecular cluster Ho(7a).

Figure S14. ^{31}P NMR spectra of Ln-POM ($Ln = Tb(5a)$, $Ho(7a)$, $Er(8a)$ and $Tm(9a)$) redissolved in D_2O solvent.

Figure S15. Plot of magnetization (M) vs magnetic field (H) for Gd(4a) POM at room temperature.

Figure S16. Thermogravimetric analysis curves of Gd(4a).

Table S1. Crystallographic table of polyanions $K_{11}[Ln(PW_{11}O_{39})_2] \cdot xH_2O$ ($Ln = Pr^{3+}$ (**1a**), Nd^{3+} (**2a**), Eu^{3+} (**3a**), Tb^{3+} (**5a**), Dy^{3+} (**6a**), Er^{3+} (**8a**), and Tm^{3+} (**9a**)) crystallized in the monoclinic system.

Polyanion	Pr-1a	Nd-2a	Eu-3a	Tb-5a	Dy-6a	Er-8a	Tm-9a
Empirical Formula	$K_{10}O_{109.50}PrP_2W_{22}$	$K_{10}NdO_{109.50}P_2W_{22}$	$K_{10}EuO_{109.50}P_2W_{22}$	$Cs_{0.50}K_9TbO_{109.50}P_2W_{22}$	$Cs_{0.50}DyK_{8.50}O_{108.50}P_2W_{22}$	$K_{10}ErO_{107.50}P_2W_{22}$	$K_{10}TmO_{110.50}P_2W_{22}$
Formula weight	6390.55	6393.88	6401.60	6435.92	6403.95	6384.90	6434.57
Crystal system	Monoclinic	Monoclinic	Monoclinic	Monoclinic	Monoclinic	Monoclinic	Monoclinic
Space group	$P2_1/c$	$P2_1/c$	$P2_1/c$	$P2_1/c$	$P2_1/c$	$P2_1/c$	$P2_1/c$
a [Å]	18.7470(6)	18.7109(7)	18.5849(8)	18.8569(15)	18.6874(6)	18.6999(9)	18.9058(6)
b [Å]	37.8100(12)	37.6178(11)	37.4594(9)	37.794(2)	37.5496(10)	37.2860(10)	37.4737(8)
c [Å]	14.1269(4)	14.1038(5)	14.0613(4)	14.0876(7)	14.0978(3)	14.0901(3)	14.1131(3)
α [°]	90	90	90	90	90	90	90
β [°]	92.533(3)	92.572(4)	92.838(3)	92.352(5)	92.233(2)	92.577(3)	92.384(2)
γ [°]	90	90	90	90	90	90	90
V [Å ³]	10003.7(5)	9917.1(6)	9777.2(6)	10031.4(11)	9885.0(5)	9814.3(6)	9990.1(4)
Z	4	4	4	4	4	4	4
ρ_{calcd} [g cm ⁻³]	4.243	4.282	4.349	4.261	4.303	4.321	4.294
μ [mm ⁻¹]	26.229	26.491	26.943	26.4513	26.924	27.092	26.667
Refelection collected	91066	62641	79788	74640	88342	79036	88565
Unique (Rint)	16343	12477	15018	14003	17140	16201	16706
Observed [$I > 2\sigma(I)$]							
Parameters	746	746	747	746	742	738	754
Gof	1.014	1.113	1.085	1.077	1.259	1.093	1.202
R [$I > 2\sigma(I)$] ^[a]	0.0575	0.0989	0.0673	0.0939	0.0743	0.0716	0.0779
Rw (all data) ^[b]	0.11825	0.2313	0.1308	0.1908	0.1323	0.1462	0.1422

[a] $R = \sum |I_F - I_Fc| / \sum |I_F|$. [b] $R_w = [\sum w(F_O^2 - F_C^2)^2 / \sum w(F_O^2)]^{1/2}$

Table S2. Bond lengths of Ln-O (\AA) for polyanions $\text{K}_{11}[\text{Ln}(\text{PW}_{11}\text{O}_{39})_2] \cdot x\text{H}_2\text{O}$ (Ln = Pr^{3+} (**1a**), Nd^{3+} (**2a**), Eu^{3+} (**3a**), Gd^{3+} (**4a**), Tb^{3+} (**5a**), Dy^{3+} (**6a**), Ho^{3+} (**7a**), Er^{3+} (**8a**), and Tm^{3+} (**9a**)).

Ln ³⁺ =	Pr	Nd	Eu	Gd	Tb	Dy	Ho	Er	Tm
Ln-O36	2.445(12)	2.46(2)	2.394(13)	2.377(12)	2.35 (2)	2.376(15)	2.343(12)	2.347(14)	2.324(16)
Ln-O37	2.436(13)	2.38(3)	2.390(15)	2.407(10)	2.35(2)	2.354(15)	2.381(11)	2.345(16)	2.340(17)
Ln-O38	2.470(12)	2.49(3)	2.414(16)	2.342(12)	2.41(2)	2.397(15)	2.321(12)	2.375(16)	2.368(16)
Ln-O39	2.467(11)	2.47(2)	2.416(14)	2.443(12)	2.40(2)	2.378(14)	2.385(11)	2.342(14)	2.351(16)
Ln-O40	2.450(13)	2.46(3)	2.407(14)	2.372(12)	2.36(2)	2.345(15)	2.337(11)	2.331(14)	2.305(16)
Ln-O41	2.446(12)	2.44(3)	2.411(16)	2.372(11)	2.37(2)	2.367(14)	2.358(11)	2.338(14)	2.338(16)
Ln-O42	2.433(12)	2.40(3)	2.406 (14)	2.406(11)	2.373(19)	2.355(15)	2.376(12)	2.316(15)	2.341(16)
Ln-O43	2.441(12)	2.39(2)	2.372(14)	2.411(11)	2.335(19)	2.340(15)	2.390(11)	2.340(13)	2.316(15)
Average	2.45	2.44	2.40	2.39	2.38	2.36	2.36	2.34	2.33

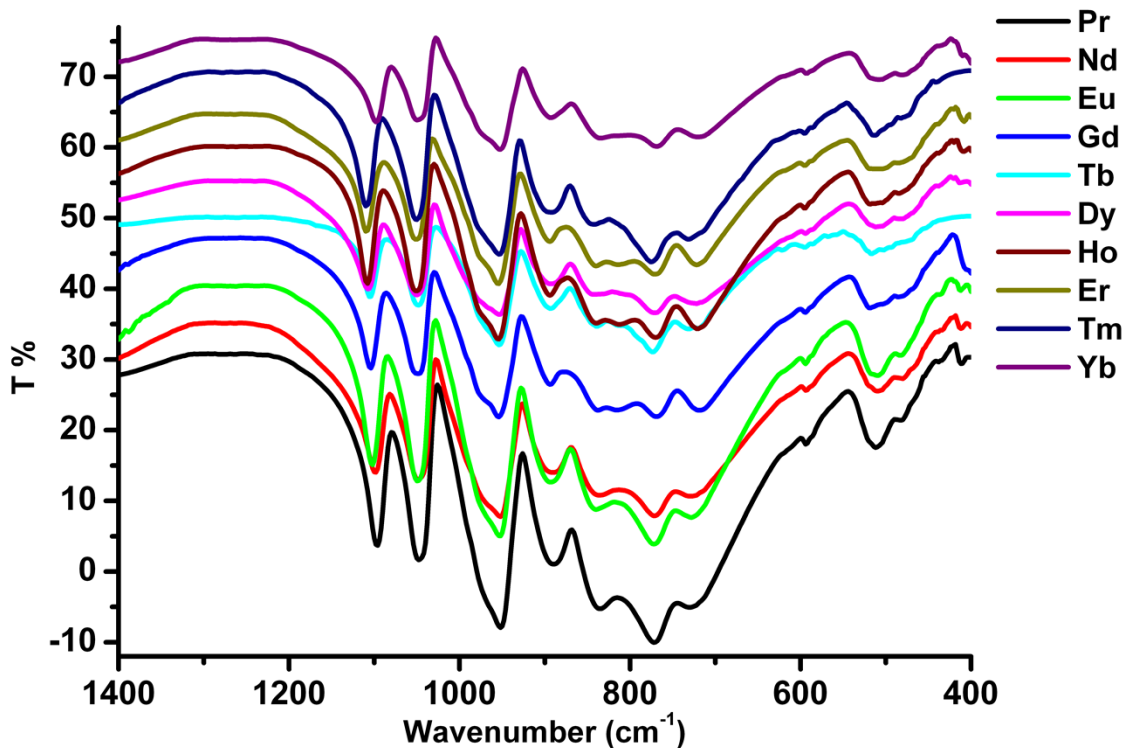


Figure S3. FT-IR spectra of molecular cluster **Pr(1a)** – **Yb(10a)** (recorded in KBr pellet, only the “fingerprint” signature of polyoxophosphotungstate is displayed).

Table S4. Vibrational frequencies of P-O and W-O bands of molecular cluster **Pr(1a) – Yb(10a)**

Sl. No.	ν_{as} (P-O)	$\nu_{as}(W-O_b)$ (W=O)	ν_{as} (W-O _b -W) (Corner sharing)	ν_{as} (W-O _c -W) (Edge sharing)
Pr³⁺(1a)	1096, 1048	951	887	836, 772, 727
Nd³⁺(2a)	1100, 1048	957	891	840, 772, 724
Eu³⁺(3a)	1104, 1048	953	891	838, 772, 727
Gd³⁺(4a)	1104, 1050	955	891	842, 770, 729
Tb³⁺(5a)	1106, 1050	951	897	838, 774, 729
Dy³⁺(6a)	1106, 1052	953	891	845, 770, 719
Ho³⁺(7a)	1110, 1050	955	893	842, 770, 721
Er³⁺(8a)	1110, 1050	955	895	842, 772, 724
Tm³⁺(9a)	1110, 1050	951	893	842, 774, 729
Yb³⁺(10a)	1197, 1049	951	893	835, 768, 718

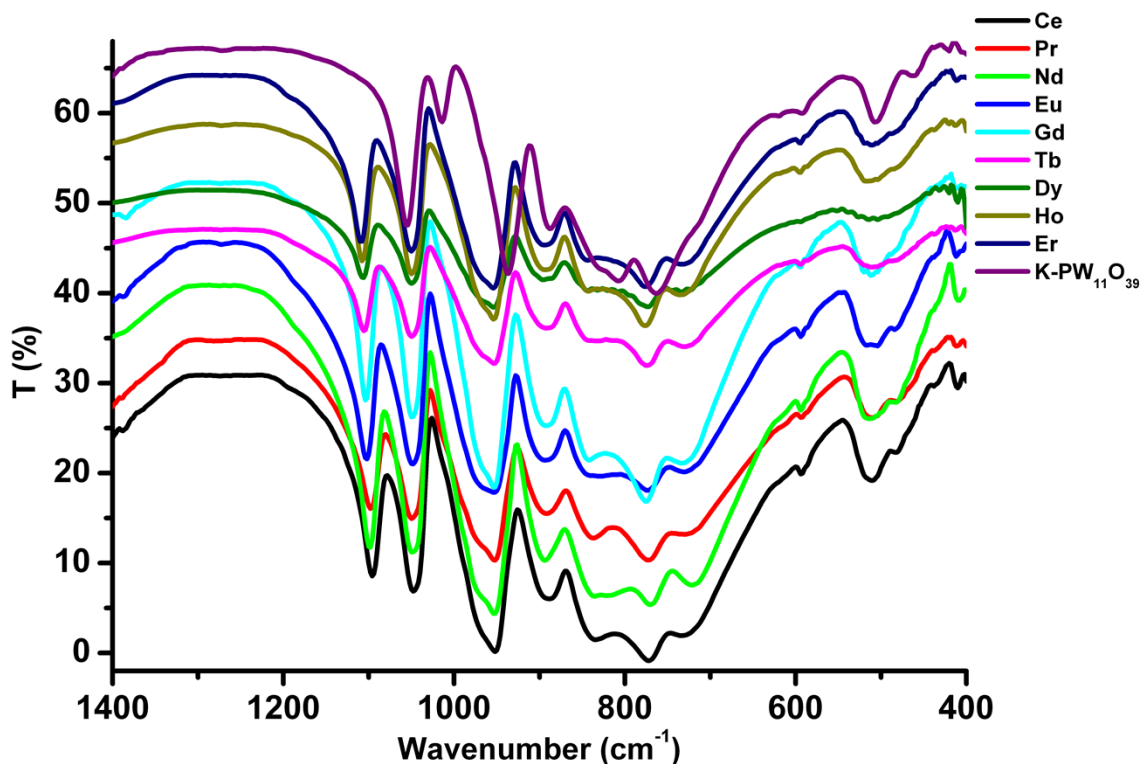


Figure S5. FT-IR spectra of Ce – Er complexes obtained from reaction of $[\alpha\text{-PW}_{11}\text{O}_{39}]^{7-}$ with lanthanoid metal salts (recorded in KBr pellet, only the “fingerprint” signature of polyoxophosphotungstate is displayed).

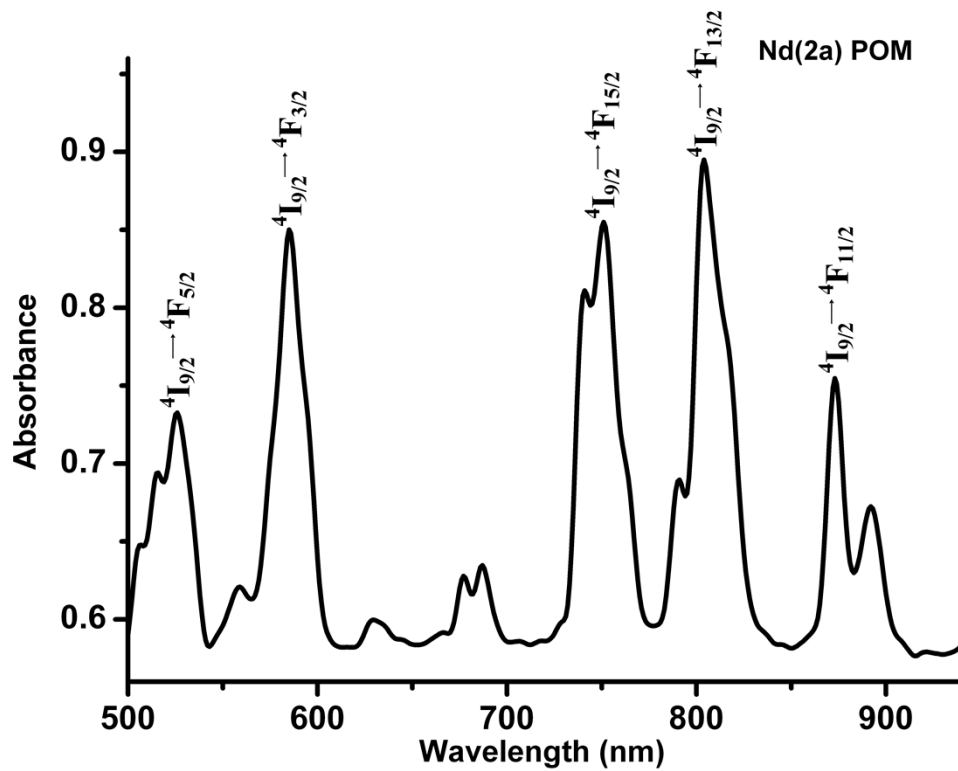


Figure S6. Solid state UV/vis spectrum of molecular cluster **Nd(2a)**.

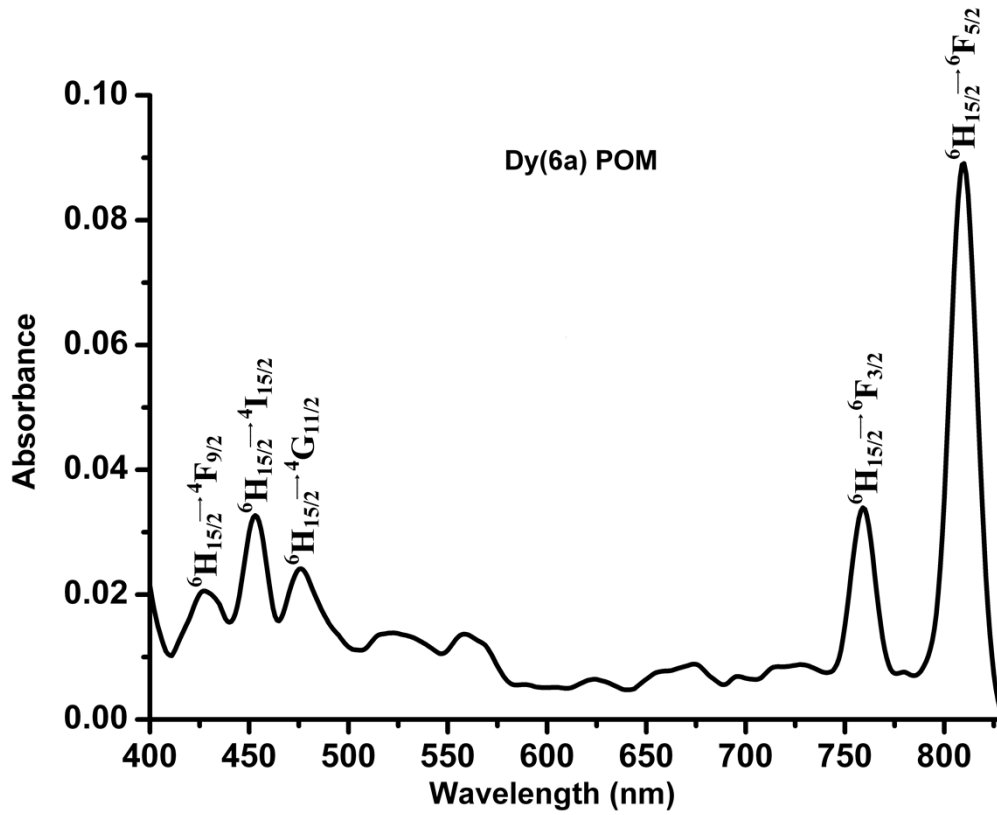


Figure S7. Solid state UV/vis spectrum of molecular cluster **Dy(6a)**.

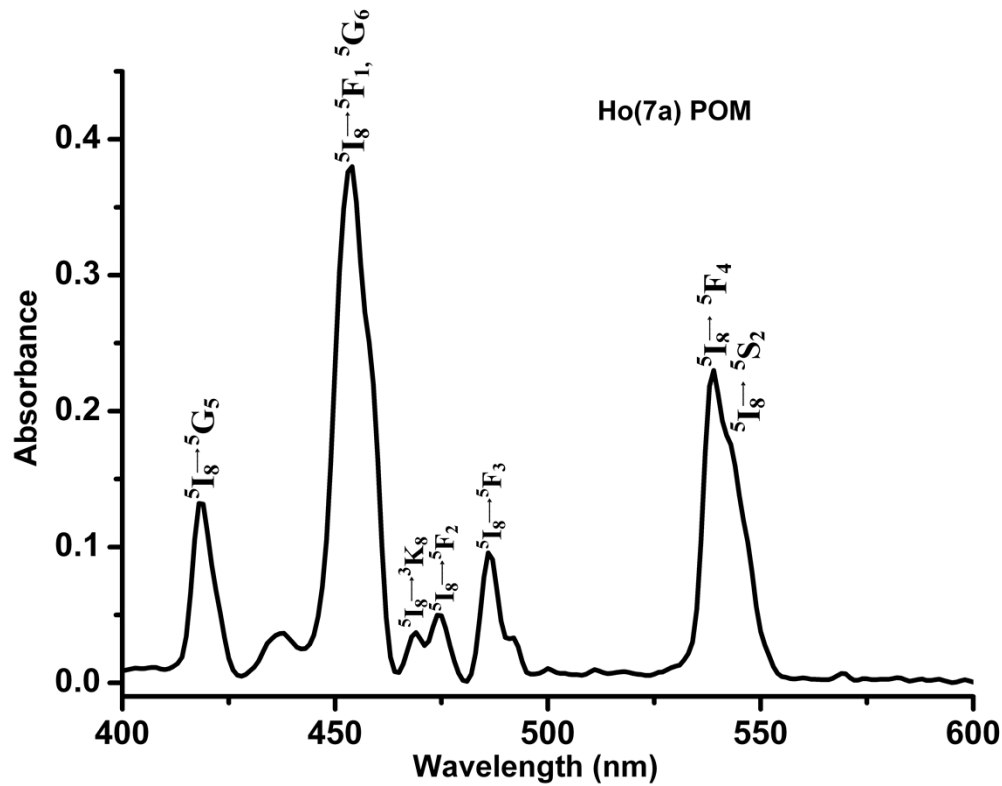


Figure S8. Solid state UV/vis spectrum of molecular cluster **Ho(7a)**.

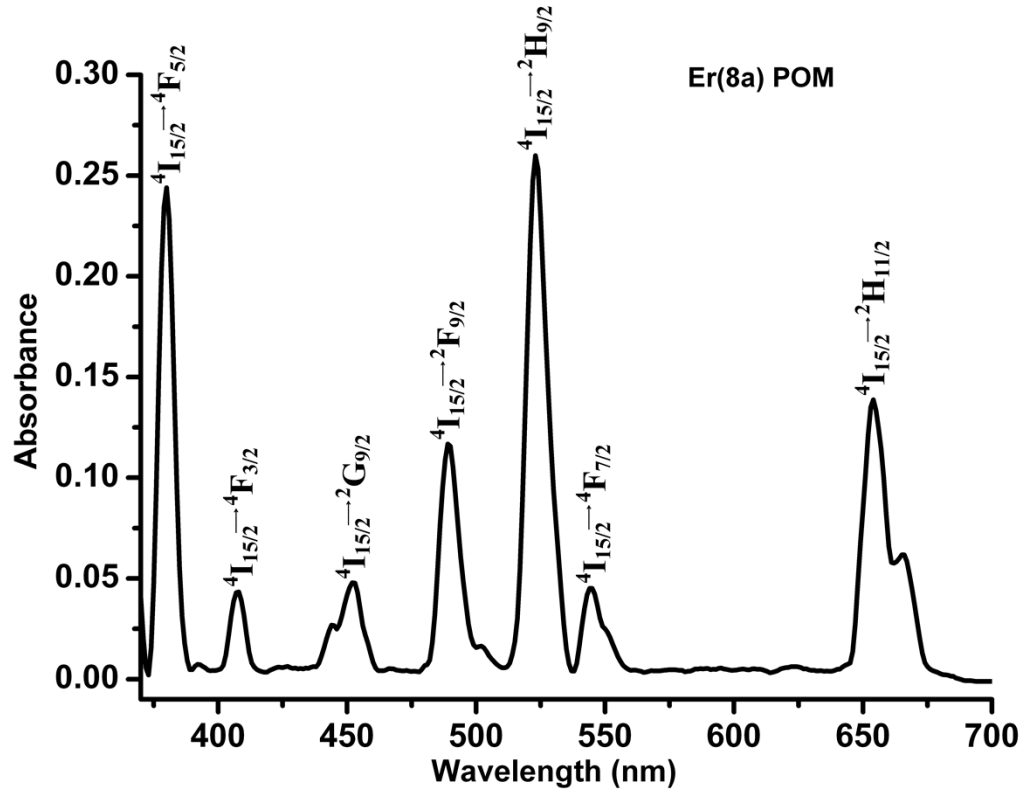


Figure S9. Solid state UV/vis spectrum of molecular cluster **Er(8a)**.

Table S10. Cathodic (E_{pc}) peak potentials, peak potential differences ($\Delta E_p = E_{pa} - E_{pc}$), formal redox potentials ($E^0 = 1/2(E_{pa} + E_{pc})$) and cathodic peak potential differences with respect to the first reduction wave of {PW11} (ΔE_{pc1}) for the electron transfer processes discussed in the text. The values are taken from voltammograms recorded at 10 mV.s⁻¹. All values are in V vs. SCE. Concentrations were 2×10^{-4} M unless otherwise stated.

pH	Species	E_{pc}	ΔE_p	E^0'	ΔE_{pc1}
3.0	Tm(9a)	-0.716	0.064	-0.684	
		-0.840	0.086	-0.797	
4.0	PW₁₁ 4×10^{-4} M	-0.714	0.076	-0.676	0.000
		-0.842	0.056	-0.814	
	Eu(3a)	~-0.834	0.200	-0.734	-0.120
		-0.934	0.128	-0.870	
	Gd(4a)	-0.842	0.200	-0.742	-0.128
		-0.928	0.138	-0.859	
	Tb(5a)	-0.836	0.186	-0.743	-0.122
		-0.926	0.084	-0.884	
	Dy(6a)	-0.846	0.196	-0.748	-0.132
		-0.926	0.130	-0.861	
	Ho(7a)	-0.834	0.184	-0.742	-0.120
		-0.916	0.126	-0.853	
	Er(8a)	-0.846	0.210	-0.741	-0.132
		-0.922	0.134	-0.855	
	Tm(9a)	-0.794	0.102	-0.743	-0.080
		-0.920	0.102	-0.869	
5.0	Eu³⁺ 8×10^{-4} M	-0.950	0.392	-0.754	
	PW₁₁ 4×10^{-4} M	-0.826	0.116	-0.768	0.000
		-0.906	0.046	-0.883	
	Eu(3a)	-0.918	0.252	-0.792	-0.092
		-1.006	0.122	-0.945	
	Tm(9a)	-0.840	0.110	-0.785	-0.014
		-0.974	0.108	-0.920	

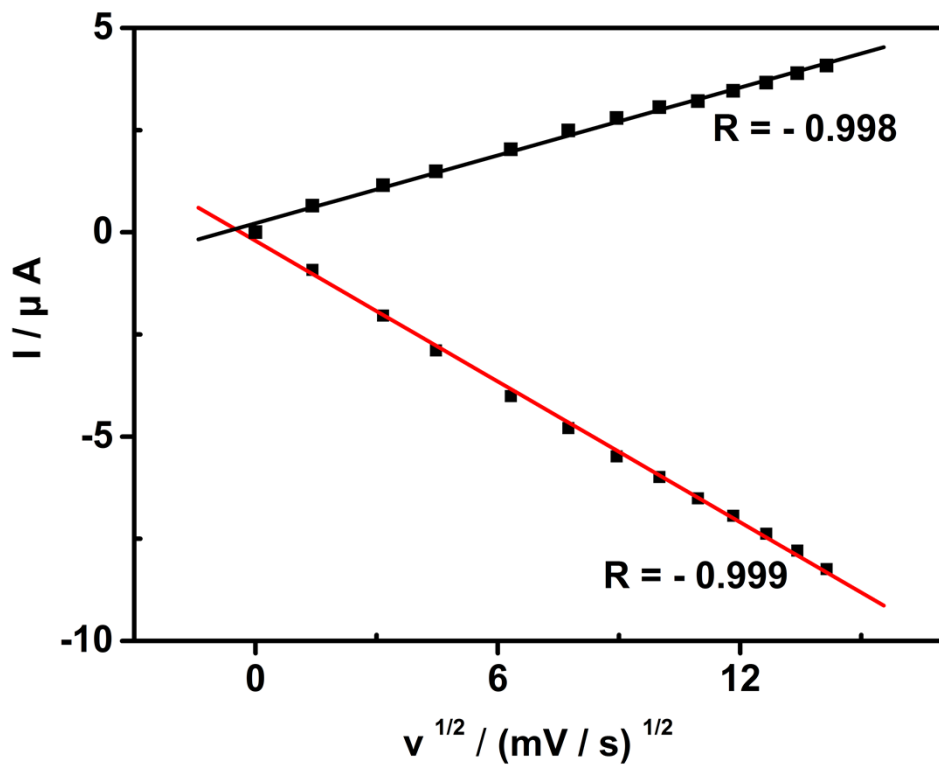


Figure S11: Dependence of the peak current on the square root of the scan rate for the most positive redox couple of a 0.2 mM Tm(9a) solution in 1 M $\text{CH}_3\text{COOLi} + \text{CH}_3\text{COOH}$, pH = 5 ($v = 2 ; 10 ; 20 ; 40 ; 60 ; 80 ; 100 ; 120 ; 140 ; 160 ; 180 ; 200 \text{ mV.s}^{-1}$).

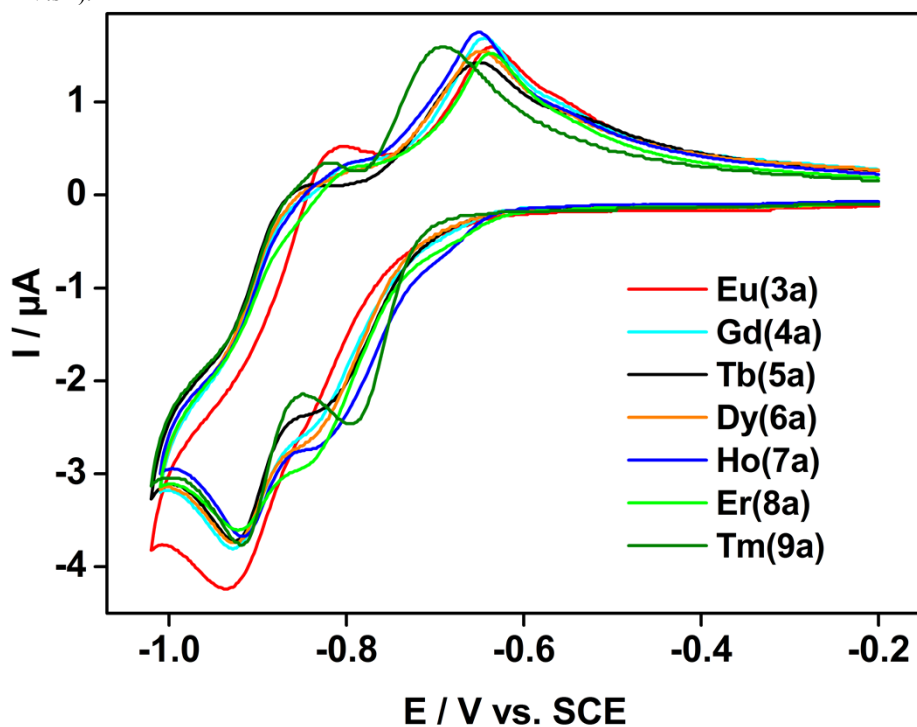


Figure S12. Comparison of the cyclic voltammograms obtained from solutions of conc. $2 \times 10^{-4} \text{ M}$ for Eu(3a) - Tm(9a) in 1 M $\text{LiCH}_3\text{COO}/\text{CH}_3\text{COOH}$, pH = 4.0, at 10 mV.s^{-1} .

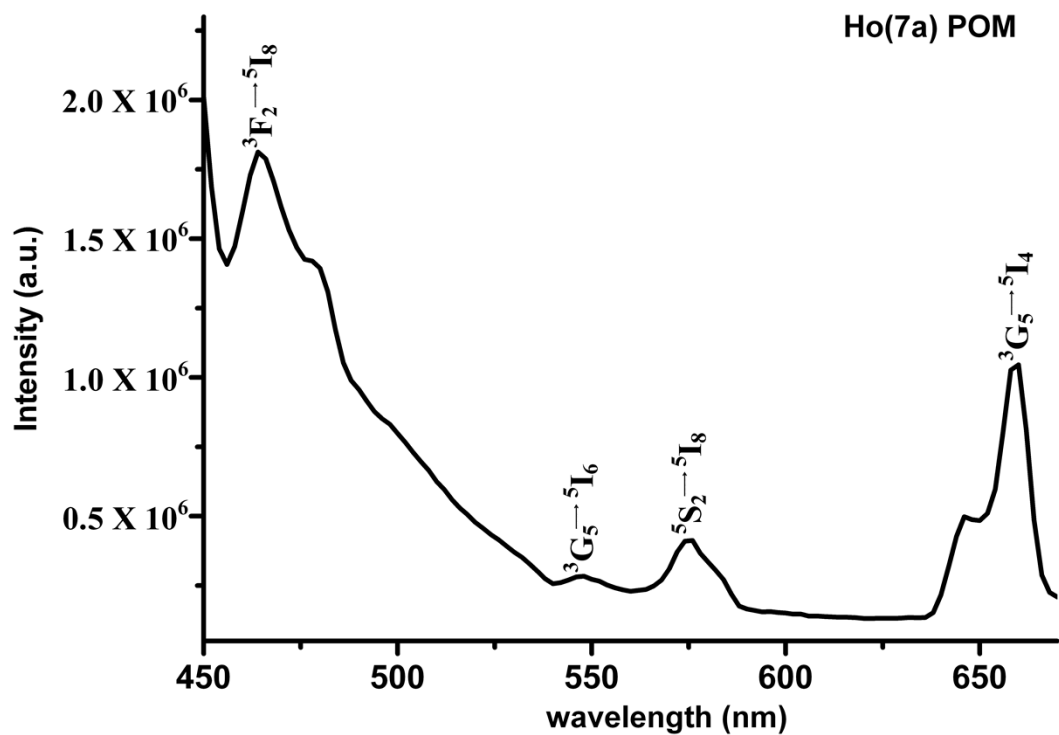


Figure S13. Photoluminescence spectrum of molecular cluster **Ho(7a)** POMs.

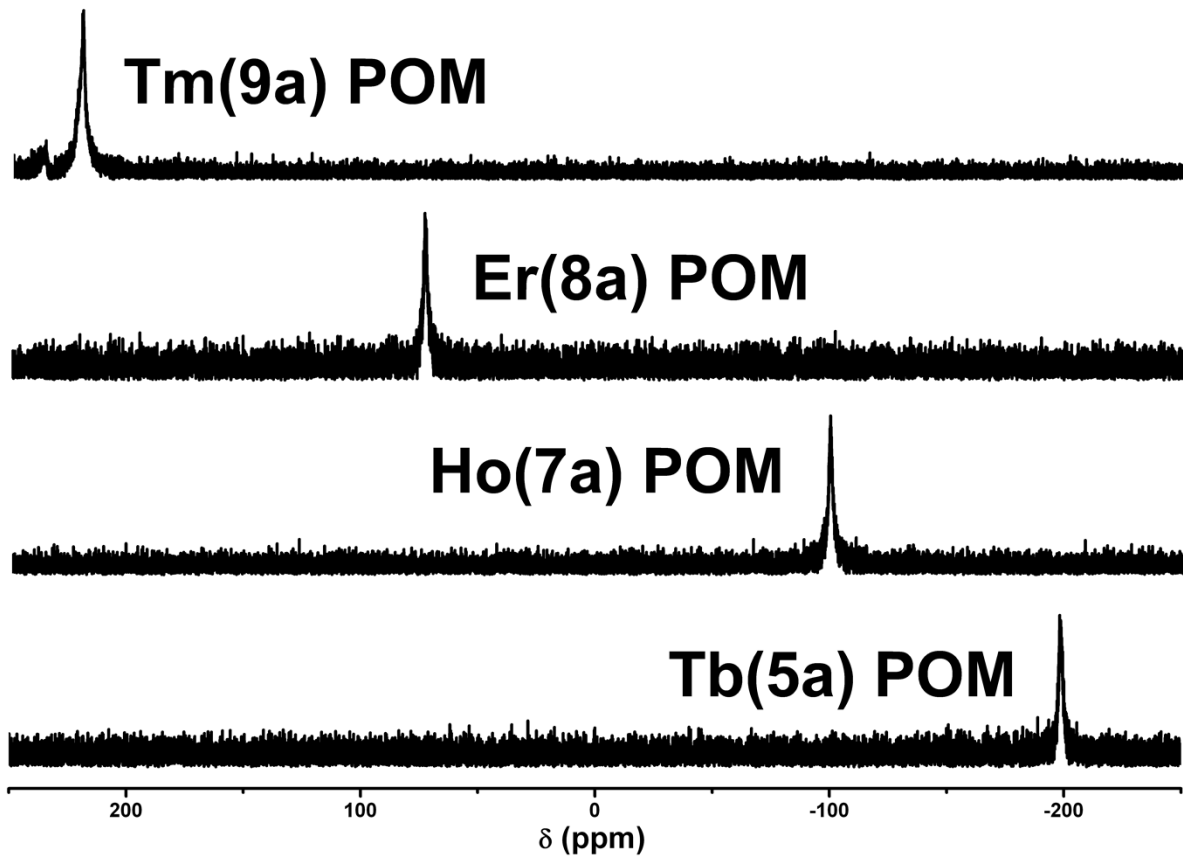


Figure S14. ^{31}P NMR spectra of Ln-POM (Ln = **Tb(5a)** top, **Ho(7a)**, **Er(8a)**, **Tm(9a)**) redissolved in D_2O solvent.

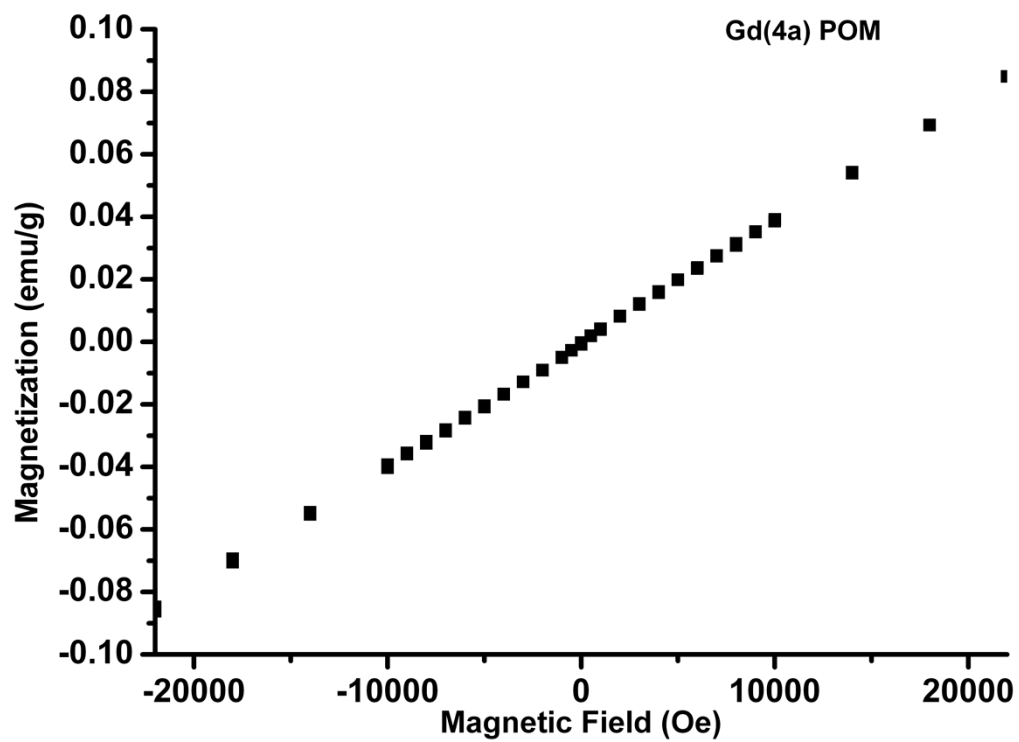


Figure S15. Plot of magnetization (M) vs magnetic field (H) for **Gd(4a)** POM at room temperature.

$$\mu_{\text{eff}} = 2.828(\chi_m T)^{1/2} \dots \dots \dots \text{(Eq.1)}$$

Where, χ_m is magnetic susceptibility and T = temperature

$$\chi_m = M/H \times \text{Molecular weight} \dots \dots \dots \text{(Eq.2)}$$

$\chi_m = 0.02515$, substitute the value of χ_m in (Eq.1)

$$\mu_{\text{eff}} = 7.75 \mu_B$$

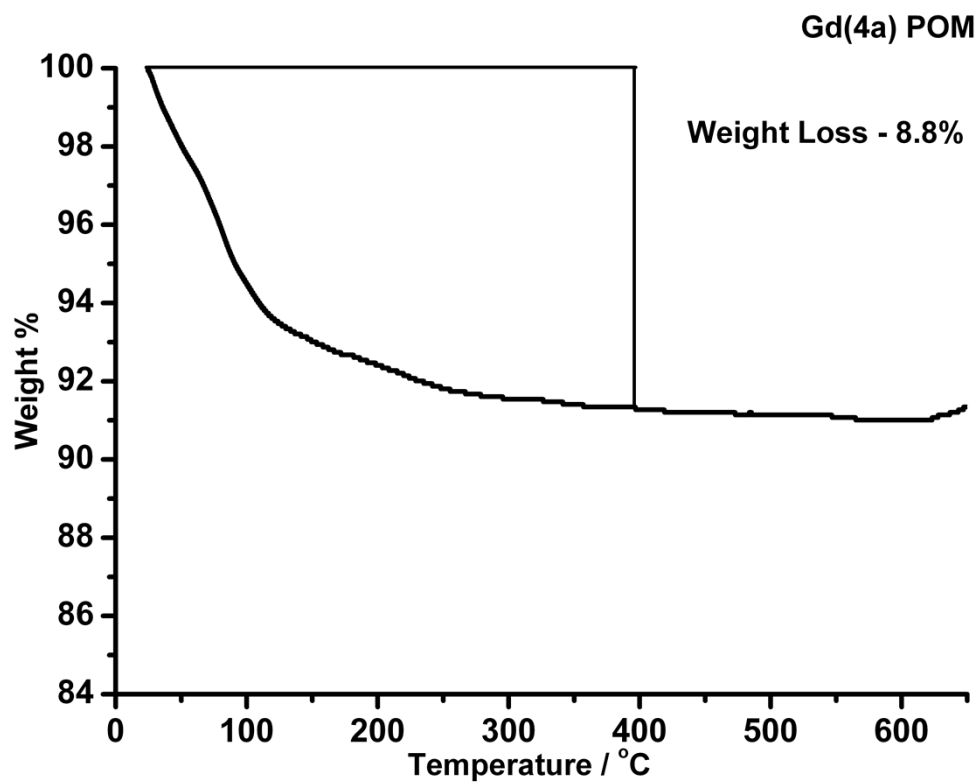


Figure S16. Thermogravimetric analysis of **Gd(4a)** POM displaying the weight loss corresponding to crystal water molecules. (Pr^{3+} (**1a**) = 5.9 %, Nd^{3+} (**2a**) = 6.9 %, Eu^{3+} (**3a**) = 7.2 %, Tb^{3+} (**5a**) = 5.9 %, Dy^{3+} (**6a**) = 7.0 %, Ho^{3+} (**7a**) = 6.8 %, Er^{3+} (**8a**) = 8.6 %, Tm^{3+} (**9a**) = 6.8 %, and Yb^{3+} (**10a**) = 7.8%).